Quadrupole Magnets for the SSC

SC-MAG 400
LBL 32790

A. F. Lietzke, P. Barale, R. Benjegerdes, S. Caspi, J. Cortella, D. Dell'Orco, W. Gilbert, M. I. Green, K. Mirk, C. Peters, R. Scanlan, C. E. Taylor, A. Wandesforde

Lawrence Berkeley Laboratory
1 Cyclotron Road
Berkeley, CA 94720

Abstract -- At LBL, we have designed, constructed, and tested four short (1m) models and six full-size (5m) models of the Superconducting Super Collider (SSC) main-ring 5 meter focusing quadrupole magnet (211 Tesla/meter). The results of this program are herein summarized.

I. MAGNET CONSTRUCTION

The eight coils in each magnet were arranged in a two-layer "cos 2θ" pattern around a circular bore (40mm) as shown in Figure 1. All coils (8-turn inner layer and 13-turn outer layer) were wound under tension (135N) with 30-strand, 1.2 degree keystone, 9.73mm x 1.062/1.268mm NbTi cable. The cable was insulated with Kapton (.05mm, 50% overlap) and fiber-glass cloth (0.1mm, impregnated with B-stage epoxy for later curing into a rigid form). Additional Kapton insulation (0.1mm) was added to each turn in the coil-end regions for insurance against scuffing damage. Fiber-glass cloth (0.1mm, B-stage epoxy impregnated) was applied to inner and outer surfaces of each end region to increase coil-end rigidity.

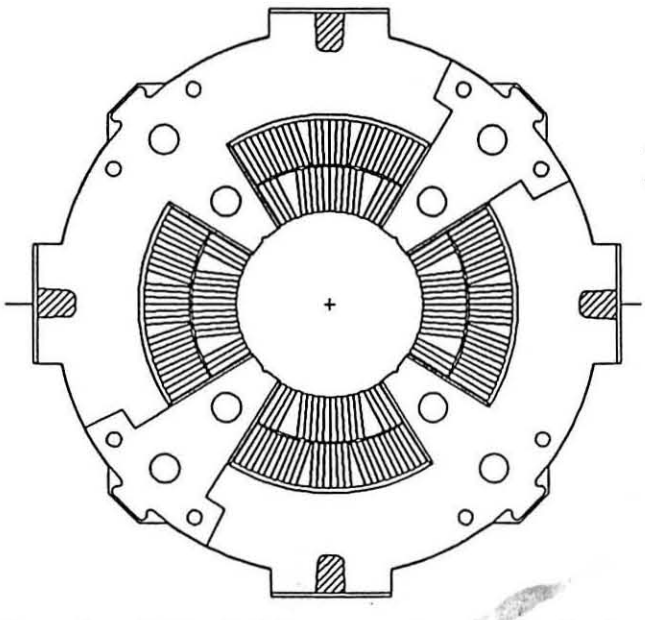

Figure 1. Collared Coil cross-section: coils, pole-pieces, collars, keys and yoke alignment tabs

Work supported by the Director, Office of Energy Research, Office of High Energy and Nuclear Physics, High Energy Physics Division, U.S. Department of Energy, under Contract No. DE-AC03-76SF00098.

Wedge-shaped copper spacers were judiciously inserted to provide a self-supporting "Roman arch" structure and maximize the quality of the quadrupole field. Voltage-tap tabs were inserted at the end of each pole-turn to facilitate the localization of quench-initiation sites.

The coil ends received special attention due to conflicting winding restrictions: 1) wide cable, 2) short radius ends (40 mm magnet bore), 3) accurate end-turn placement for field accuracy [3], 4) adequate margin and 5) good mechanical support for the cable. End-spacers were designed with a "constant perimeter" shape (for tight, easy winding). They were empirically altered slightly after experience with the first models (to improve winding conditions); the pole end-islands were altered to provide gentler, more controlled bends in the high-field region (to improve cable support near the inter-layer splice).

The coils were placed in a fixture and compressed (50-90 MPa azimuthally and 7-12 kN axially) to final size and heated (130C) to polymerize the epoxy. This made each coil self-supporting enough to ease removal from the winding fixture and facilitate assembly on a temporary mandrel. Layer-to-layer insulation was augmented by installation of pre-shaped Kapton and Teflon sheets between layers. Similar layers enhanced the insulation between the coils and their support structures.

The coil end-regions (outside the iron yoke) were clamped either by stainless-steel C-shells (the 1st two magnets: QSC 401 & 402) or an aluminum collet (all subsequent models). The radial clamping force was transmitted to the coil assembly through an annular G-10 spacer. Two glass-fiber orientations were tested: axial-azimuthal (QSC 401 &402) and double-transverse (all subsequent models).

The coil assembly was aligned, compressed and supported by many symmetrical, interlocking collaring plates (18mm thick Al or SS; preassembled into 146mm long, pinned "collar-packs"). An internal collaring mandrel was used to improve conductor placement and bore diameter accuracy. The collar-packs were aligned by four collar tabs which fit into key-way grooves machined into the iron "yoke-blocks" (see Figure 2). The horizontal tabs carried the weight of the collared coils (unless shims were installed to clamp the collared coil with the yoke-blocks). The vertical tabs controlled the horizontal centering. Structural analysis of this collaring system was done by D. Dell'Orco [4].

Each yoke-block (460 mm long) was assembled from round iron laminations (267mm x 1.52mm), compressed, fastened with pins, and glued for rigidity. Azimuthal alignment of each yoke-block was provided by keys inserted thru accurately machined openings in the shell. Weld shrinkage from the two full-length axial welds locked this alignment to the shell. The keys were removed after welding and the holes were sealed for vacuum integrity. The end-to-end twist was less than 3mradians for all 5m magnets

Magnetic coil alignment was controlled by the collars, which were keyed to the yoke-blocks, which were keyed to the shell and locked in place at the welding of the shell.

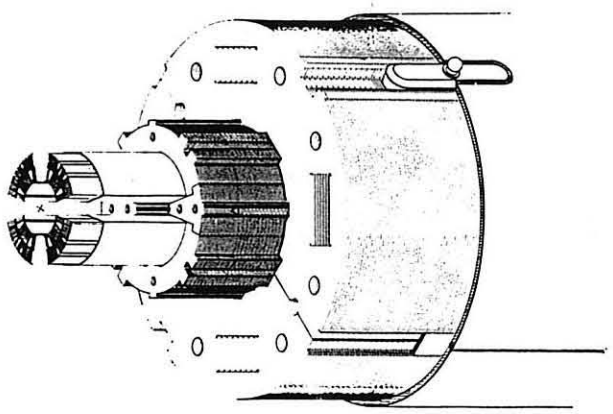

Figure 2 : Cold-mass section: shell, yoke, collars, and coils

Both magnet-ends were immobilized (relative to the welded shell) and compressed axially by applying a force (20 kN) between each magnet end-piece and its associated end-clamp. Further details of the design can be found in Reference 1.

Construction extended over a period of nearly two years and there were numerous small changes made in the design and fabrication techniques. Design parameters that were varied in this series of twelve magnets (10-virgins, 2-retests) include: magnet end-region radial-clamping system, end-region immobilization system, collaring material, collaring pressure, collaring mandrel length, collaring mandrel hardness, collar/yoke friction, magnet length, conductor manufacturer, and curing/collaring procedures

II. TEST PROCEDURES

Each magnet was installed in a horizontal cryostat. A thermal cycle was initiated with the measurement of the average room-temperature quadrupole gradient, and relative multipole purity (from Fourier analysis of the rotating, 1 cm radius coil signals) [5]. These pre-cooling measurements were needed to establish a baseline for subsequent warm-cold correlations. High-current testing commenced after cool-down (1Atm, boiling helium) and system validation tests were completed satisfactorily. For cold, pre-training magnetic measurements, the magnet was energized (5000A @16A/s) three times before 3000 A plateau measurements were made. On-the-fly measurements were taken to determine the instantaneous magnetic multipole fields.

Magnet training quenches were produced by increasing the current at a steady rate (normally 16 A/s) until a quench was detected. Current extraction operations were initiated after a quench had propagated a distance that depended upon a balance of conflicting desires: 1) accurate quench-initiation localization (> 1 magnet length), 2) quench propagation or maximum MIITs studies (no extraction, immediate free-wheeling power supply), or 3) minimizing the time required to recover for another attempt.

The magnet current, and strain-gage load-cells (16 in a 1m magnet, 24 in a 5 m magnet), each in a balanced bridge arrangement [7], were monitored on-the-fly as rapidly as the hardware permitted (<3 sec/complete set in a 5m magnet) When a quench was detected, the magnet current, coil voltages and differential voltage-tap signals (11/quadrant, mostly pole turns) were recorded (typically @ 5kHz (2 kHz or less for maximum MIITs) for quench-origin studies [8]

Training proceeded at 4.3K (1Atm, boiling helium) until a plateau was achieved or sub-cooling (2.5K) was used to accelerate the process. Most of the short (1m) magnets were also trained at 1.8K (10.44kA, max.) to determine the robustness of the design and help identify potential weak areas. Ramp-rate sensitivity of the plateau current was tested with a range of up-ramps (1A/s to 1kA/s).

Quench-heaters were minimally tested by measuring the delay between the quench-heater excitation, and observable quenching elsewhere in the magnet. A minimum quenching delay of 60 ms was observed. Parametric dependencies were investigated only for the first magnet to have quench-heaters (QCC 402). Computation of the MIITs (1E-6*$\int$I*Idt), a quick, nonlinear estimate of the relative temperature of the hottest spot in the magnet, was used to compare various magnet protection methods. The MIITs are inversely related to the overall quench propagation speed away from the initiation location and can vary from coil to coil and magnet to magnet. Maximum MIITs resulted when a quench was triggered by energizing a spot-heater located at the outer mid-plane (where the absolute slowest quench propagation is expected).

Magnetic measurements were repeated after training to estimate the pre-training/ post-training, correlations. Axial scans of full-size magnets were used to determine their effective magnetic length when cold and trained.

A thermal cycle was terminated by returning the magnet to 300K. Subsequent thermal cycles were used to 1) finish procedures that were unfinished, or 2) repeat procedures (training and magnetic measurements) needed to estimate the effect of thermal cycling.

III. TEST RESULTS

Figure 3 shows the 4.3K, 16A/s training behavior of the 10 quadrupoles. LBL training was in a 1Atm static helium

bath; BNL training occurred in a pressurized, forced-flow cryostat. The magnet was horizontal in all tests. All magnets required some training to reach a plateau current. Training quenches started predominantly in the inner coil, while plateau quenches started predominantly in the outer coil (as expected [1]). Long (5 meter) magnets (Figure 4b) trained as fast as short (1 meter) magnets (Figure 4a). .

Performance improved substantially between the first and last magnets. The last two magnets required no training below 7170A. Later magnets generally started at higher current (exceptions: QCC 404 and QCC 406) and required fewer quenches to achieve and maintain plateau levels (exception: QCC 404 started lower but trained parallel to QCC 403).

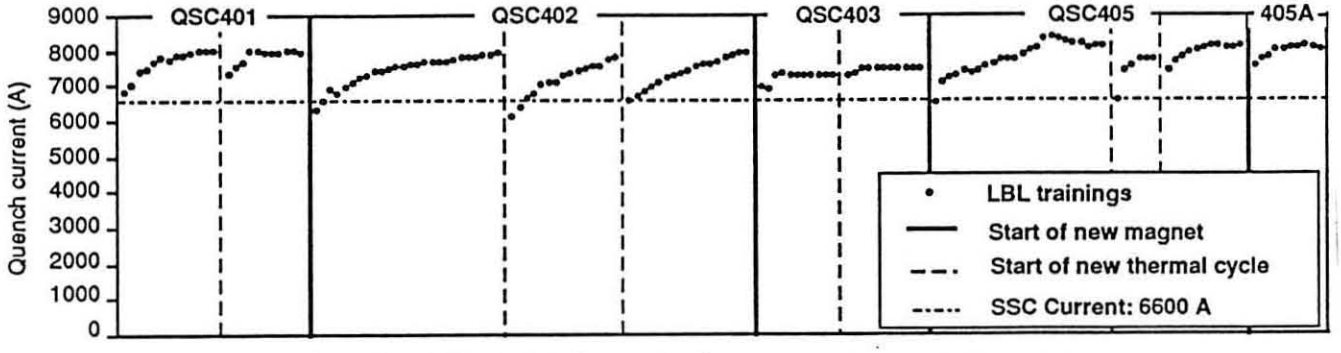

Figure 3b: 4.3 K, 16A/s Composite Training History (Long 5m Magnets)

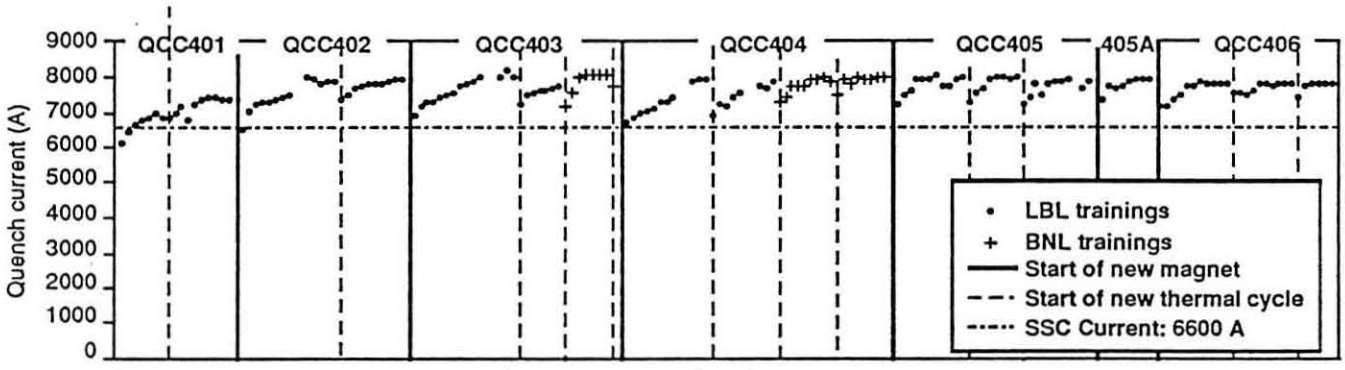

Figure 3a: 4.3 K, 16A/s Composite Training History (Short 1m Magnets)

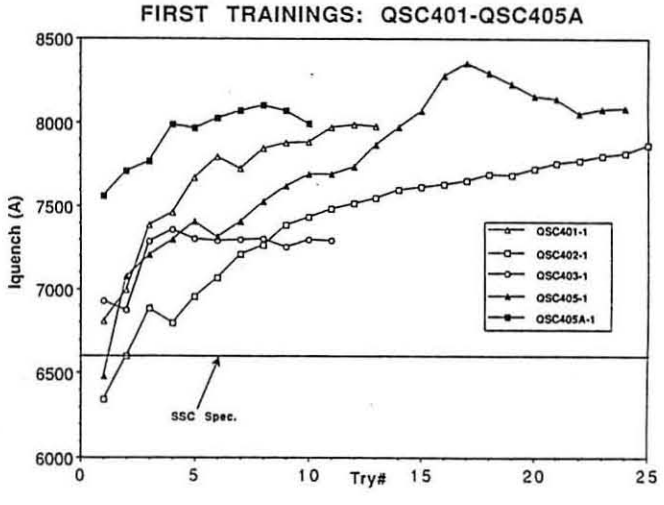

Figure 4a: 4.3K , 16A/s 1st Training Comparison (Short Magnets)

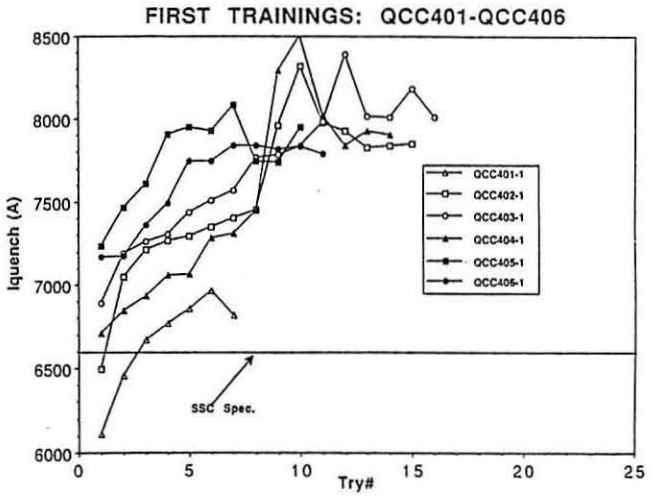

Figure 4b: 4.3K , 16A/s 1st Training Comparison (Long Magnets)

Magnets that had lower plateau currents required fewer quenches to attain plateau: QSC403 (7300A) vs. QSC405 (8080A), and QCC 406 (7840A) vs. QCC 405 (8080A). Sub-cooling (<2.5 K) dramatically reduced the number of quenches needed to reach the plateau current.

Re-training: All magnets had to be retrained (Figure 4c) after being warmed to room temperature. Subsequent thermal cycles started higher and trained faster (some more dramatically than others). Clamping the collared coil firmly in the yoke did not significantly change the retraining (compare QCC 405A with QCC405, Figure 4c)

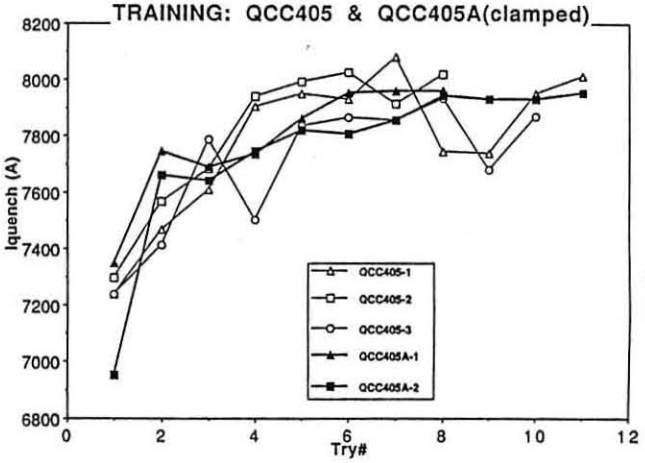

Figure 4 c: 4.3K , 16A/s Re-Training on Thermal Cycling

Quench propagation: Figure 5 illustrates a typical quench initiation in a long straight section and its propagation speed, until it exits into adjacent end regions. The ever-present heating contribution was removed by subtracting a polynomial (a*t^2.5+b*t+c) that best met three conditions: zero starting and exit offsets, with uniform propagation speed in the middle of the magnet. A temporary speed dip occurs at each end.

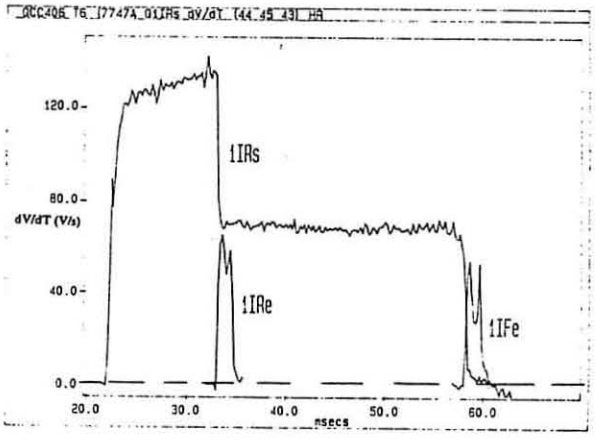

Figure 5: Typical Quench Initiation and Propagation, 5m Magnet (1 IRs: Quad 1, Inner, Return, Side).

Quench-origins (Q-O's): All training quenches originated in the pole turn. Each magnet showed a characteristic pattern of quench-origins (Figure 6a,b,c)

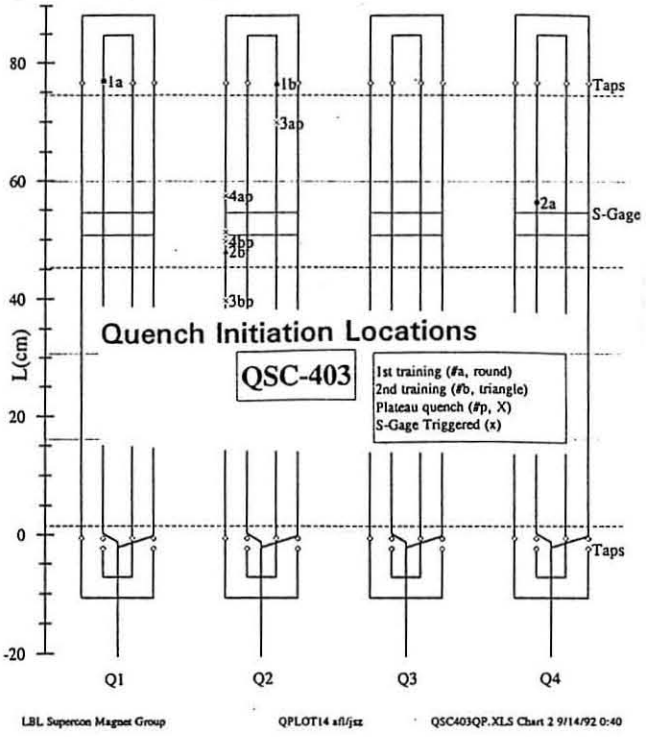

Figure 6a: Quench-Origins for QSC403 Trainings:

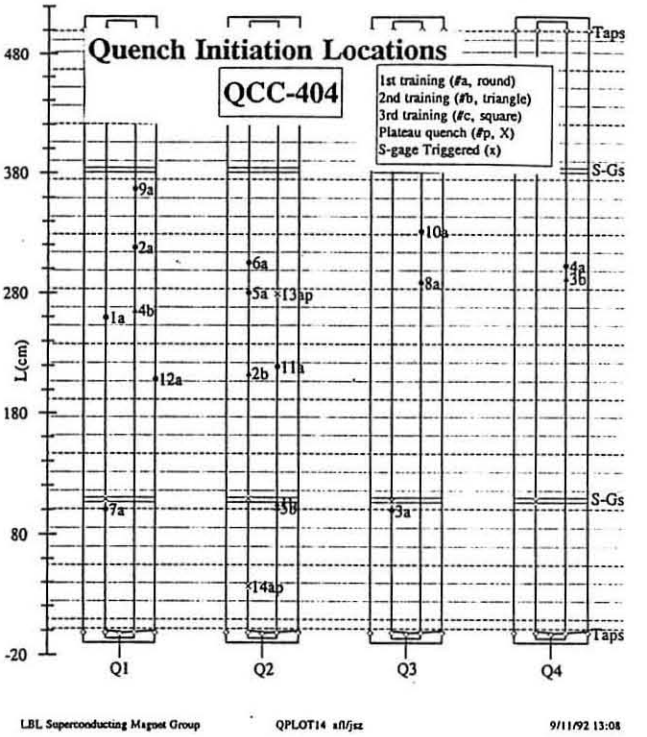

Figure 6b: Quench-Origins for QCC404 Trainings

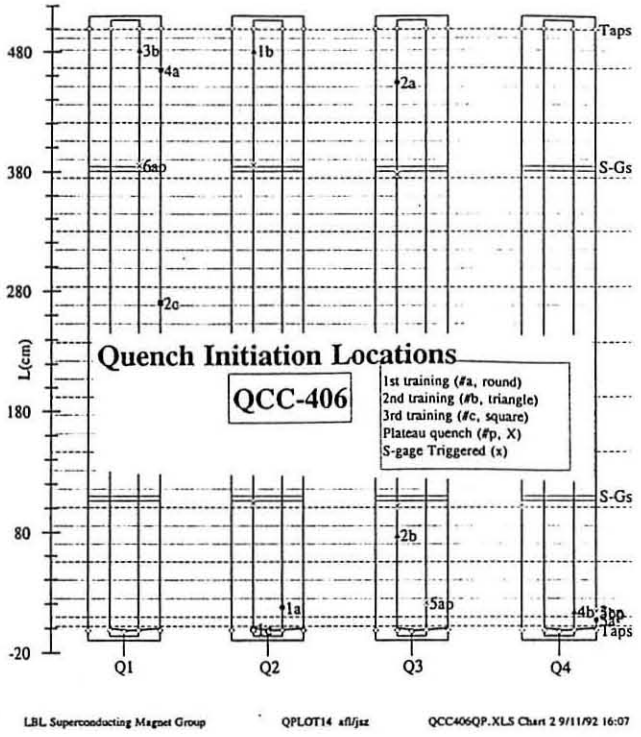

Figure 6c: Quench-Origins for QCC406 Trainings: 1st (Circles), 2nd (Triangles), 3rd (Squares).

Figure 6a,b,c shows a schematic of the eight pole-turns. The axial locations of the quench-origins (Q-O's) are shown relative to voltage taps, strain-gages, collar-pack boundaries,, hard-mandrel edges, and the inter-layer ramp-splice (bottom of figure. QSC 403 (Figure 6a) exhibited most of its quench-origins (Q-O's) near the return end in the 2nd quadrant, while QCC404 (Figure 6b) revealed a band of Q-O's near the middle, and QCC 406 (Figure 6c) suffered most of its Q-O's near its ends. This axial non uniformity was usually preserved over thermal cycles but usually with a change in quadrant (QSC 403 being an exception).

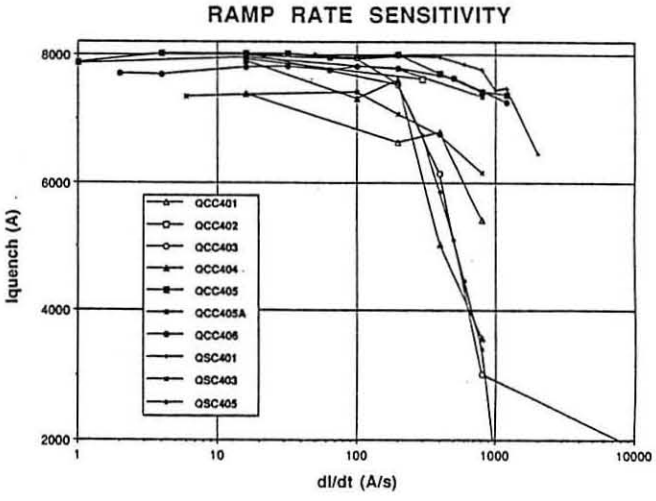

Figure 7: Ramp-rate Dependence of Plateau Current (all Magnets)

It was extremely rare for a magnet to repeat any particular Q-origin. Exceptions (QSC401 and QSC402) were later discovered to have end-clamp design oversights (improperly machined ramp-kink groove, compressed by G-10 in the high-shrinkage direction, compressed by a low-shrinkage stainless-steel clamp); QSC 403 corrected these oversights and showed a dramatic reduction in training. Exception QCC406 is believed to have a broken strand (Quad4, Outer,-layer Feed-side, Feed-end)

Ramp-rate sensitivity varied from magnet to magnet (Figure 7). The low ramp-rate sensitive magnets had either been collared more than once (QSC 401, QCC 405) or used a new conductor surface treatment (QCC406). They also exhibited higher maximum MIITs (Figure 8).

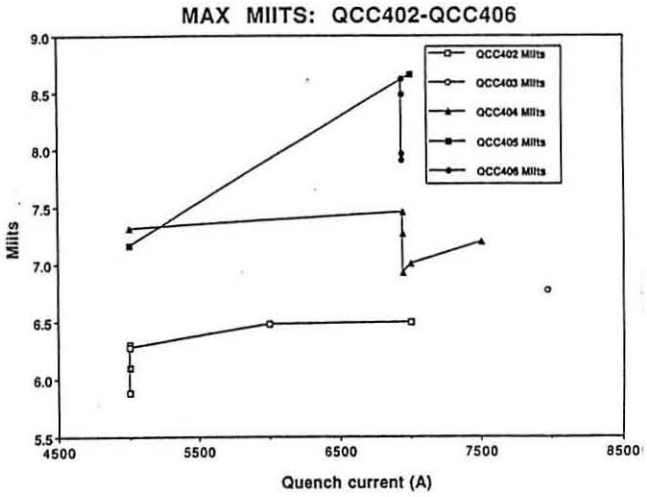

Figure 8: MIITs for Mid-plane Triggered Quenches

Strain-gage history: Events like collaring, yoke-clamping, skinning, welding, and thermal cycles are dramatically visible in the historical strain-gage record [7]. Cool-down loss with stainless-steel collars (30-40MPa) are 6-8 times the cool-down loss observed with aluminum collars; consequently stainless-steel collared magnets must be collared to higher pressures in order to maintain the same operating margin when cold.

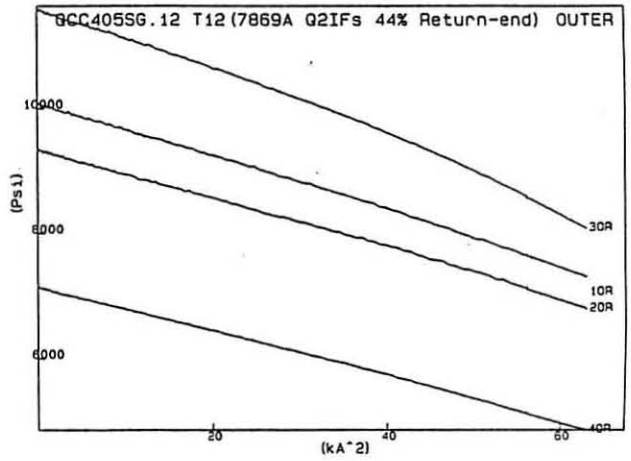

Figure 9a: Typical Strain-gage Excitation Response

Strain-gage response: After training, most magnets produced a linear response to the Lorentz load (Figure 9a). In spite of considerable variations in the initial stress (correlated to the measure coil sizes), substantial pole pressure remained at 8000 A. QCC406 (Figure 9b) was an exception. It suffered an unexpected amount of creep and arrived for testing with unusually low pole pressures. Some locations were unloaded above 6 kA. No obvious effect on training was observed.

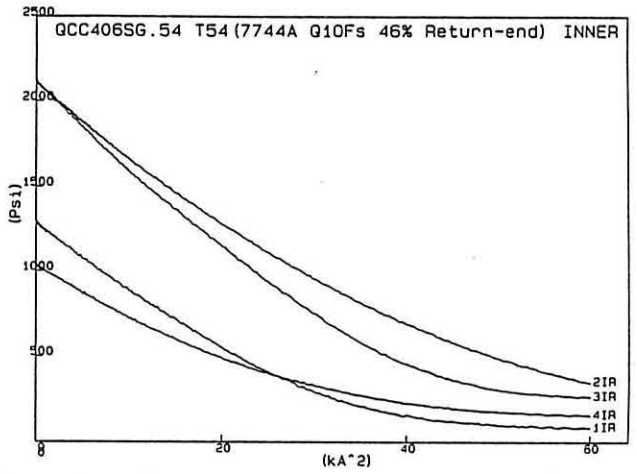

Figure 9b: Strain-gage Response for Low Initial Stress

Strain-gage virgin ramp: Ramping into virgin territory (exceeding previous excitation levels, Figure 9c) revealed a steeper unloading rate (i.e., lower coil stiffness), especially in the outer coils. This "mechanical" training characteristic repeated itself on subsequent thermal cycles and may be related to the manner in which these magnets "forgot" their training after being warmed to 300K. While ramping to 1st quench, several load cells revealed an anomalous stiffening (slower change in pressure vs. Lorentz load) prior to quench initiation (Figure 9d). Quench-initiation was often localized to the quadrant which exhibited the largest anomaly.

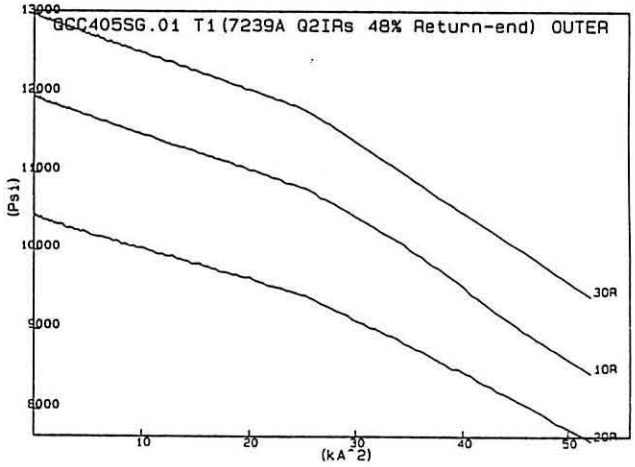

Figure 9c: Strain-gage Response Entering Virgin Territory

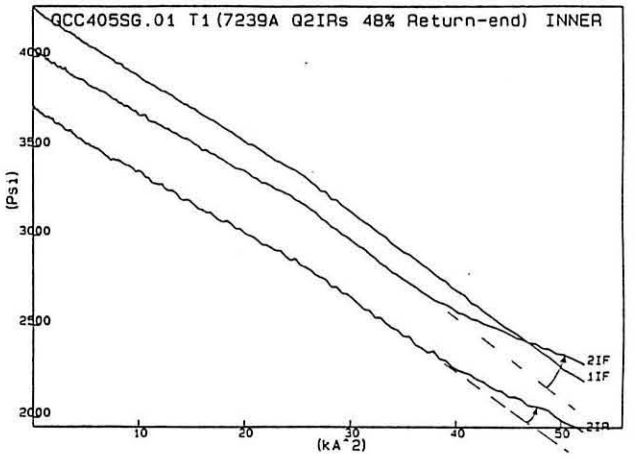

Figure 9d: Strain-gage Response Near Quenching

Magnetic measurements: The gradient transfer function (33.3 Tesla/m/kA @ 6500 A) was repeatable over thermal cycles (Figure 10a) and from magnet to magnet (Figure 10b). Its axial variation (Figure 10c) showed a very uniform central region and produced an integral magnetic gradient of 172.8 Tesla/kA. The higher-order multipoles (Figure 11a,b) were generally smaller than SSC acceptance requirements (except for the 1st magnet) and showed very small decays [5] The warm-cold correlations were reproducible (Figure 12a,b) to within $0.5 * 10^{-4}$ units (warm).

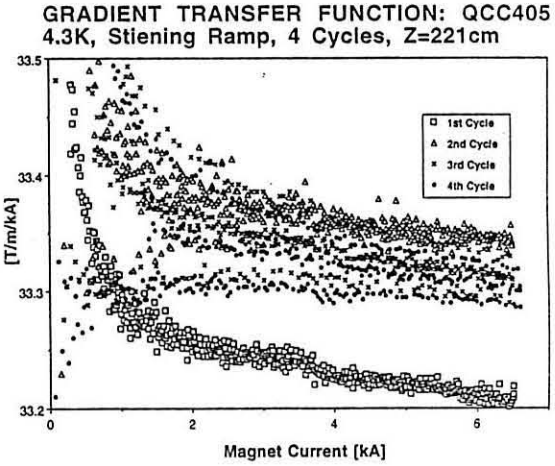

Figure 10a: Typical Gradient Transfer Function Responses for Several Thermal Cycles, Z = 220 cm

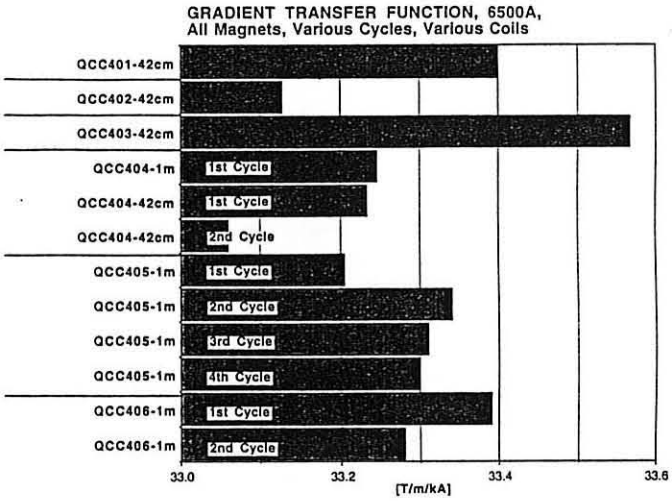

Figure 10b: Gradient Transfer Function at 6500A for Several Magnets

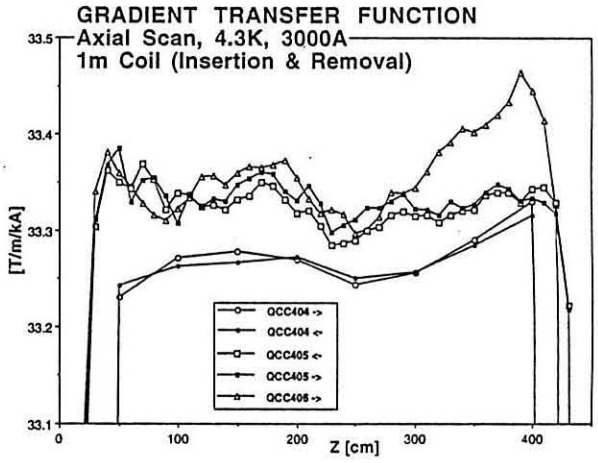

Figure 10c: Axial variation of the Gradient Transfer Function for Several Magnets

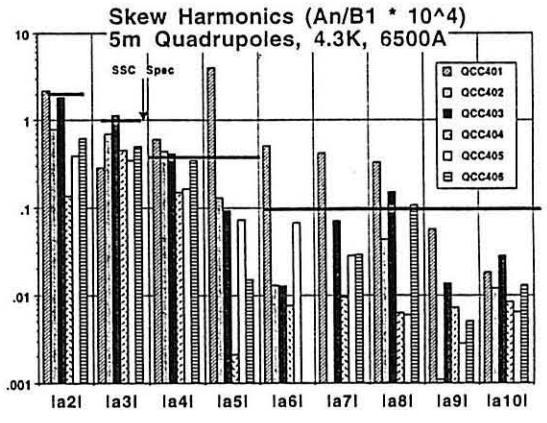

Figure 11a: Normalized Skew Mulitpole Components (E-4 units) for Several Magnets

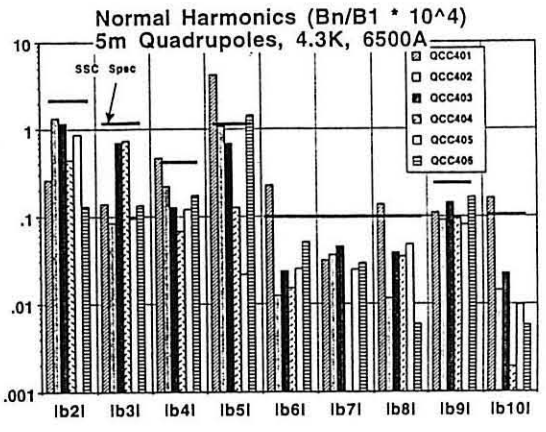

Figure 11b: Normalized Normal Multipole Components (E-4 units for Several Magnets

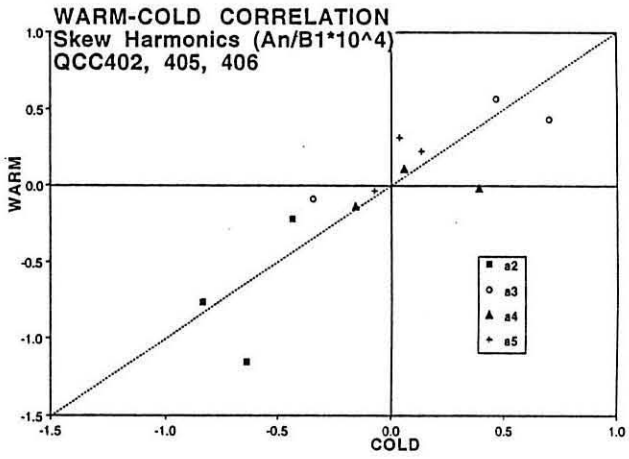

Figure 12a: Typical Warm-Cold Correlation of Skew Multipoles

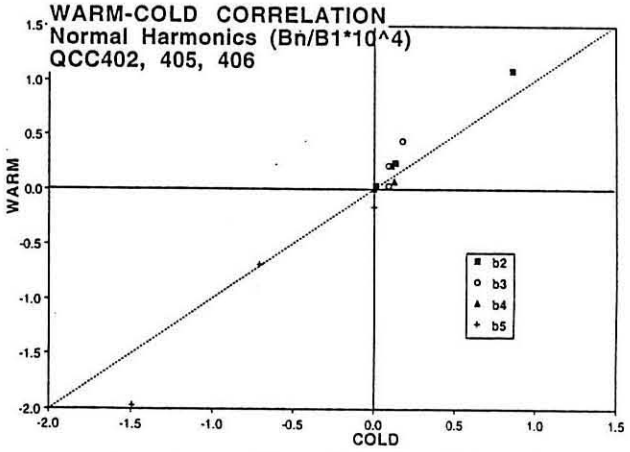

Figure 12b: Typical Warm-Cold Correlation of Normal Multipoles

IV. DISCUSSION

The importance of adequate coil clamping was dramatically supported by the improved training when the end-region cold-clamping pressure was maintained (magnets after QSC402). Several repetitive quench-initiation locations were eliminated. How much pressure is enough, is still questionable in view of QCC406's Lorentz unloading, yet second best training.

The issue of optimum yoke-collar friction is also unclear. QSC405A (re-collared, welded and clamped in the yoke) trained the fastest of all magnets. Unfortunately, uncollaring may be no guarantee of restoring virgin conditions. QCC404, on the other hand (lightly clamped), trained much more slowly than magnets built to slide. (QCC403, 405, 406). QCC405A (QCC405 clamped) trained no better than earlier training's; the training only moved to a new location.

The larger "virgin compliance observed during the first excitation, suggests that the cable/collar system has some freedom to deform under Lornetz loading. The stiffening observed just prior to quenching suggests that some parts of the system resist this deformation and may constitute a source of stored energy capable of triggering quenches. Lack of memory retention after thermal cycling suggests that restoring forces exist that are strong enough to restore a somewhat "virgin" state during some part of the cycling process; but the movement of the quench-origins to new locations implies that the magnet is "reset" to a different "virgin" condition.

The inverse correlation between Miits and ramp-rate sensitivity is additional evidence that dI/dt-triggered down-ramp quenching can decrease the maximum cable temperature. after quenching

The repeatability and axial uniformity of the gradient transfer function is a testament to the accuracy of the bore diameter. Whether this accuracy can be maintained without using a collaring mandrel was not tested. The low multipole content suggests accurate azimuthal placements (probably aided by the attempts to cure coils to size).

Correlation's between warm and cold multiple measurements suggests that warm measurements can be predictive to within at least 0.5×10^{-4} of the fundamental.

V. SUMMARY

Ten pre-prototype magnets including six 5 m models were designed, constructed and tested at LBL in order to provide proof of principle demonstrations of the design proposed to meet SSCL operational requirements. Except for modest training, the magnets performed very well and proved to be self-protecting. Some design flaws (e.g., inadequate end-clamping and pole shimming) were identified and corrected sufficiently that the later magnets exceeded specifications. The last two 1m models and all the 5m models have been (or are expected to be) reinstalled in cryostats at the SSC Laboratory, retested and used to achieve various milestones in their program. The SSC Laboratory has contracted with a commercial vendor to design, construct and test a series of production prototypes based on this design.

VI. REFERENCES

[1] C. E. Taylor, et al; *IEEE Trans. on Mag.*, vol. 27, No. 2, March 1991.

[2] S. Caspi, "The 40mm SSC Arc Quadrupole - Magnetic Design," SC-MAG-314, LBID-1677, November 1990.

[3] S. Caspi, M. Helm, and L. J. Laslett, "Magnetic Field in the End Regions of the SSC Quadrupole Magnets," MT-12 Conference, Leningrad, USSR, June 23-28, 1991.

[4] D. Dell'Orco, "Finite Element Analysis of the QC Quadrupole Magnet for the Superconducting Supercollider," LBL-29600, October 1989.

[5] M. I. Green, et al; *IEEE Trans. on Mag.*, vol. 24, No. 2, March 1988.

[6] M. A. Green, P. J. Barale, R. W. Benjegerdes, W. S. Gilbert, M. I. Green, R. M. Scanlan, J. Sopher, and C. E. Taylor, "Measurements of Magnetization Multipoles in Four Centimeter Quadrupoles for the SSC," Cryogenic Engr. Conf., Huntsville, AL, June 11-14, 1991.

[7] J. M. Cortella, A. Devred, A. Wandesforde, "Mechanical Properties of Full-Scale Proptotype Quadrupole Magnets for the SSC" (SC-MAG 401, also in these proceedings).